Synthesis and Characterization of Terpolymer Adsorbents Using Photopolymerization: Investigation of Heavy Metal Adsorption Capacity

Gözde MURAT SALTAN [1]*

[1] Department of Chemistry, Faculty of Arts and Science, Manisa Celal Bayar University, Yunus Emre, 45140 Manisa, Türkiye

Abstract

In this study, poly(allylphenol-co-methylmethacrylate-co-vinyl imidazole) (PAMV) terpolymer adsorbents were synthesized using the photopolymerization method with 1-vinyl imidazole, methyl methacrylate, and 2-allylphenol monomers. UV-A lamps with an average length of 400 nm were used in the study, which was carried out with benzophenone photoinitiator at room temperature and in a solvent-free environment. Structural and surface analyses of PAMV polymers obtained using different mole ratios 1H-nuclear Magnetic Resonance (1H-NMR), Fourier-Transform Infrared Spectroscopy (FT-IR), X-Ray Photoelectron Spectroscopy (XPS), Scanning Electron Microscopy-Energy Dispersive X-Ray (SEM-EDX) and thermal characterization were performed using thermogravimetric (TG) methods. Inductively Coupled Plasma Mass Spectrometry (ICP-MS) was used for adsorption studies. Optimization conditions of pH 2, 4, 6, 8, and 10 were determined. According to the obtained results, the pH range in which the adsorbents operate at maximum efficiency is between 6-10. Although many different metals have been studied, the holding capacity of the obtained polymeric adsorbent on cadmium, chromium and mercury metal ions is quite remarkable.

Keywords: Terpolymers, Adsorbtion, Photopolymerization, Characterization

Fotopolimerizasyon Yöntemi ile Terpolimer Adsorbentlerin Sentezi ve Karakterizasyonu: Ağır Metal Adsorpsiyon Kapasitelerinin İncelenmesi

Öz

Bu çalışmada, 1-vinil imidazol, metil metakrilat ve 2-allilfenol monomerleri ile fotopolimerizasyon yöntemi kullanılarak poli(allilfenol-ko-metilmetakrilat-ko-vinil imidazol) (PAMV) terpolimer adsorbanlar sentezlenmiştir. Benzofenon fotobaşlatıcı ile oda sıcaklığında ve solventsiz ortamda gerçekleştirilen çalışmada ortalama 400 nm uzunluğunda UV-A lambaları kullanıldı. Farklı mol oranları kullanılarak elde edilen PAMV polimerlerinin yapısal ve yüzey analizleri [1]H-Nükleer Manyetik Rezonans (^{1}H-NMR), Fourier-Transform Infrared Spektroskopisi (FT-IR), X-Işını Fotoelektron Spektroskopisi (XPS), Taramalı Elektron Mikroskopisi-Enerji Dağılımlı X-Işını (SEM-EDX) ve termal karakterizasyonu termogravimetrik (TG) yöntemleri kullanılarak gerçekleştirildi. Adsorpsiyon çalışmaları için İndüktif Eşleşmiş Plazma Kütle Spektrometresi (ICP-MS) kullanılmıştır. Optimizasyon koşulları pH 2, 4, 6, 8 ve 10 olarak belirlenmiştir. Elde edilen sonuçlara göre adsorbanların maksimum verimde çalıştığı pH aralığı 6-10 arasındadır. Birçok farklı metal üzerinde çalışılmış olmasına rağmen elde edilen polimerik adsorbanın kadmiyum, krom ve civa metal iyonları üzerindeki tutma kapasitesi oldukça dikkat çekicidir.

Anahtar Kelimeler: Terpolimer, Adsorpsiyon, Fotopolimerizasyon, Karakterizasyon

*Corresponding Author: gozde.murat@cbu.edu.tr
Gözde MURAT SALTAN, https://orcid.org/0000-0002-9097-3716

1. Introduction

Water, which plays a very important role in our body, is being polluted with highly toxic heavy metals because of the rapid increase in human population and industrialization. Metals such as mercury (II), cadmium (II), chromium (III), lead (II) and copper (II) can be counted at the beginning of the industrial and human-induced water pollution by heavy metals [1-3]. Various techniques, such as oxidation [4], coagulation [5], solvent extraction [6], chemical precipitation [7], reduction [8], ion-exchange [9] and adsorption [10] have been applied to separate, remove and enrich these types of pollutants from clean water or aqueous solutions. However, these techniques can be expensive, polluting and time consuming. Therefore, both the production of the selected adsorbents and the technique used for heavy metal removal from water should be inexpensive, environmentally friendly and practical. Adsorption technique is a widely used method for the removal of toxic metals from water, wastewater or aqueous solution due to its availability, environmental behavior and low cost [11,12].

In today's industry, there is a constant race to develop fast, cheap and effective materials with superior properties against the increasing costs and lack of raw materials. The use of terpolymers is one of the most important ways to obtain superior materials from past times. In the literature, it can often be seen that adsorbents, which are relatively cheap and have a high sorption percentage, are obtained from terpolymers. In most of these studies, it was used as a resin [13,14] or chelating [15,16] terpolymer in batch separation method with ion exchange function. In these studies, the preparation of terpolymers is in the form of chemical reactions using co-reagents, temperature and solvents. However, the importance of environmentally friendly methods such as solvent-free, temperature-free and cheaper photopolymerization is increasing [17].

Norrish Type I photoinitiators fabricate the free radicals over an α-cleavage. Besides, Norrish Type II photoinitiators form free radicals via hydrogen abstraction, which can be obtained from a coinitiator or intramolecular process. It should also be noted that the original Norrish Type II cleavage reaction works with intramolecular hydrogen abstraction followed by a C-C bond cleavage that does not give rise to any radical species that can initiate free radical polymerization. There are photoinitiators which are among the most common components used in photoinitiating systems in the last decade including, tertiary amine and contain aromatic carbonyl groups such as thioxanthone, organic dyes, quinones, and benzophenone groups. Among them, benzophenones are frequently used [18,19]. On the other hand, Scheme 1 shows the reactive centers and the polymerization mechanism.
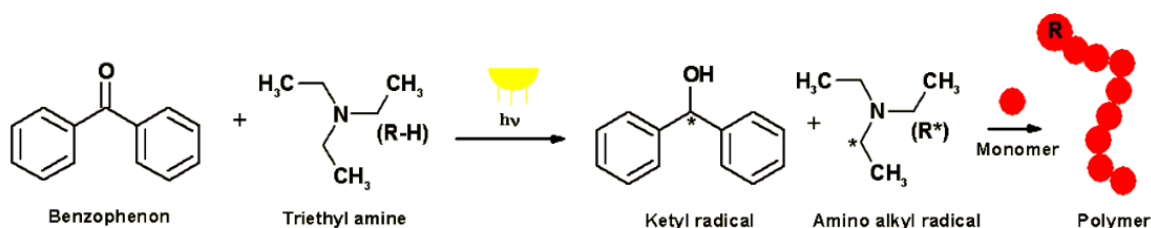
Scheme 1. Type II photoinitiation mechanism with benzophenone and hydrogen donor

It has been reported that terpolymers prepared with chelating monomer show better retention against some metal ions at different electrolyte concentrations, pH ranges and time intervals [20]. Many polymeric ligands containing functional groups are known to be used to remove heavy metal ions from aqueous solutions. It has been reported that poly(methacrylic acid) complexes with zinc (II), cobalt (II) calcium (II), while poly(vinylimidazole) strongly interact with lead (II), copper (II), cadmium (II) and cobalt (II) [21].

The aim of this study is to prepare PAMV adsorbents under ambient temperature conditions in a solvent-free environment via photopolymerization using methyl methacrylate, allyl phenol and vinyl imidazole monomers. The method used in the study differs from its similar in the literature in that it is environmentally friendly, inexpensive and short. The structures of the synthesized adsorbents were identified using different techniques such as SEM-EDX, XPS, FT-IR, ^{1}H-NMR and TG/DTA. The obtained PAMV adsorbents have been involved to adsorption by batch separation method with respect to change in pH.

2.   Materials and Methods

2.1.   Materials

Methyl methacrylate (contains ≤30 ppm MEHQ as inhibitor, 99%, Sigma-Aldrich), 2-Allylphenol (98%, Sigma-Aldrich), 1-Vinyl Imidazole (≥99%, Sigma-Aldrich), Benzophenon (for synthesis, Sigma-Aldrich), Diethyl ether (anhydrous, ACS reagent, ≥99.0%, contains BHT as inhibitor, Sigma-Aldrich), Methanol, (ACS Reagent, ≥99.8%, Sigma-Aldrich), diethyl ether (contains 1 ppm BHT asinhibitor, anhydrous, ≥99.7%, Sigma-Aldrich).

Photo Lamps: Osram Ultra Vitalux 300w-e27; Lamp voltage 230 V, Rated wattage300 W, Construction voltage 230 V; Rated voltage 230 V, 315 nm (UV-B) 3.0w, 400 nm (UV-A) 13.6w.

ICP multi-element standard solution IV-1.11355.0100(23 elements in diluted nitric acid, 1000 mg/L (106ppb): Ag, Al, B, Ba, Bi, Ca, Cd, Co, Cr, Cu, Fe, Ga, In, K, Li, Mg, Mn, Na, Ni, Pb, Sr, Tl, Zn, MERCK)

2.2. Instrumentation

XPS analysis was performed with a Thermo Scientific instrument and this device's library was used to interpret the analysis results (USA). All SEM images were obtained using a field emission scanning electron microscope Carl Zeiss Sigma 300 VP under high vacuum at a voltage of 15.0 kV with a working distance of 6.0 mm. 1H-NMR measurements were recorded in DMSO-d6 with Si(CH3)4 as an internal standard, using an Agilent Premium Compact 600 MHz, 14.1 Tesla instrument. FT-IR spectra were recorded on a Perkin Elmer FTIR Spectrum One-B spectrometer (USA). In addition, attenuated total reflection (ATR) apparatus was used for this analysis. Thermal gravimetric analysis (TG), derivative thermogravimetry (DTG) and differential thermal analysis (DTA) were performed on the TA Instruments TA/TGA with a heating rate of 10 °C/min under nitrogen flow. Molecular weights were determined by gel permeation chromatography (GPC, Viscotek VE3580 RI detector, UK) instrument equipped with a Waters styragel column (HR series 2, 3, 5E) with THF as the eluent at flow rate of 1 mL/min and a Waters 410 differential refractometer detector.

All measurements of adsorbents were performed using 7700x Agilent-ICP-MS system. The operating conditions for ICP-MS are listed in Table1. A Thermo Fisher Scientific combined electrode pH meter was used to control the pH of metal-mix solutions. The mixture was sonicated using ultrasonic bath.

Table 1. Operating conditions of the ICP-MS device

Plasma power	1.3 kW
Auxiliary flow rate	0.87 L min^{-1}
Sampler orifice (nickel)	1.1 mm
Acquisition mode	Peak-jumping
Dwell time	0.1 s
Number of measurements per peak	3
Plasma flow rate	15 L min^{-1}
Nebulizer flow rate	1 L min^{-1}
Skimmer orifice (nickel)	0.7 mm
Number of sweep	100
Acquisition time	60s

2.3. Photoinduced Synthesis of Poly(allylphenol-co-methylmethacrylate-co-vinyl imidazole) (PAMV)

Allylphenol (Ap) was first added to vacuum-argon-treated two-necked balloons under argon atmosphere. 1% benzophenone was added according to the total mole amounts of monomers as a photoinitiator. Subsequently, Vinyl imidazole (VIm) and auxiliary monomer Methylmethacrylate (MMA) were added to the reaction medium. (Note: Before polymerization, the monomers were purified with an alumina column to remove their stabilizers.) Finally, triethylamine, used as the H-donor, was added to the medium in a catalytic amount and the

mixture was mixed in an argon atmosphere and under pre-prepared UV-A/UV-B lamps. The amounts used in the synthesis method are clearly indicated in Table 2. When the specified times are completed for the polymerization, the polymers are removed from the reaction medium by precipitation in cold ether. If the polymer liquid is viscous, precipitation is performed after dilution with some methanol. The solid polymers obtained are left to dry in a vacuum oven at 30 ºC for one day. The representative view of the synthesis and synthesis scheme are given in Figure 1 and Scheme 2, respectively. There was no precipitation of the $PA_3M_1V_1$ derivative, polymerization did not progress in this experiment. This is thought to be because the hydroxyl group on the allyl phenol group acts as a radical scavenger. There are studies examining the radical scavenging potentials of phenolic compounds with theoretical and experimental methods and finding similar results [22, 23].

Table 2. Molecular weight distribution of polymers and experimental conditions

Monomer ratios (moles) Ap:MMA:VIm	Monomer amounts	Photoinitiator Quantities (Total Mol 1.0%)	H-Donor	Rxn (Hour)	M_n (kg/mol)	PDI (M_w/M_n)	Conversion (%)
$(PA_1M_1V_1)$ 1:1:1	VIm: 0.85 mL (0.88 g) — MMA:1 mL (0.94 g) — Ap:1.22 mL (1.26 g)	2.8×10^{-4} mole (0.05 g)	0.015 mL	6	17700	2.1	60
$(PA_1M_3V_1)$ 1:3:1	VIm: 0.85 mL (0.88 g) — MMA:3 mL (2.82 g) — Ap:1.22 mL (1.26 g)	4.69×10^{-4} mole (0.08 g)	0.015 mL	6	18200	2.4	70
$(PA_1M_1V_3)$ 1:1:3	VIm: 2.55 mL (2.64 g) — MMA:1 mL (0.94 g) — Ap:1.22 mL (1.26 g)	4.69×10^{-4} mole (0.08 g)	0.015 mL	6	15700	2.3	75
$(PA_3M_1V_1)$ 3:1:1	VIm: 0.85 mL (0.88 g) — MMA:1 mL (0.94 g) — Ap:3.66 mL (3.78 g)	4.69×10^{-4} mole (0.08 g)	0.015 mL		N/A		

Photopolymerization method was used in the study to synthesize polymer adsorbents. The lamps selected for this technique should be able to radiate in the UV-A/UV-B region. This radiation can be in the wavelength ranges of 315 nm-400 nm (UV-A) and 280 nm-315 nm (UV-

B). As it is known, benzophenone shows maximum absorption in the UV-B region, and the lamps used in the study produce at least 6 W power in this region.
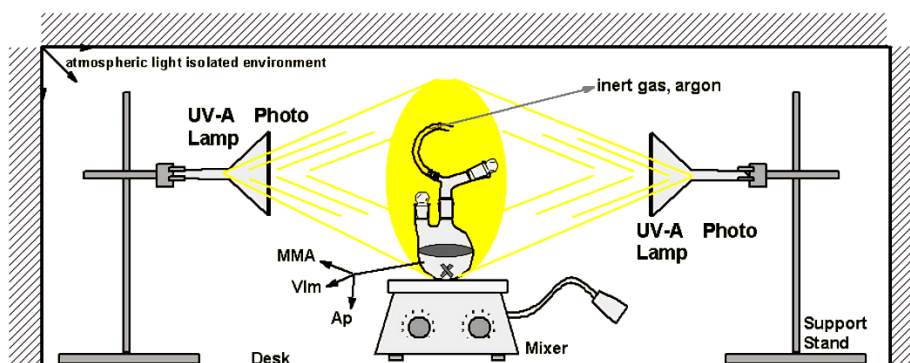
Figure 1. Schematic representation of the reaction medium
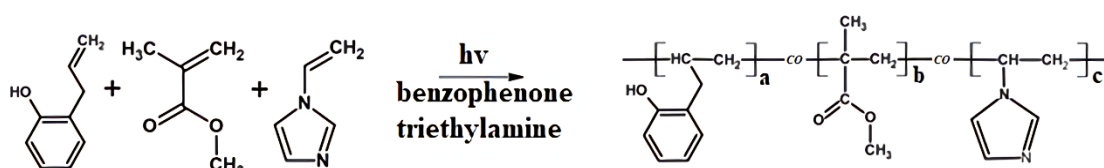
Scheme 2. Synthesis of PAMV terpolymers

2.4. Adsorption Experiment

A 100 ppb intermediate stock standard was prepared from a commercially available 106 ppb standard multi-element solution. Since the pH parameter will be evaluated, solutions were prepared from the intermediate solution with pH=2, 4, 6, 8, and 10. Batch-type adsorption experiments were carried out by adding 25 mL of each pH solution to 50 mL falcon tubes. 10 mg of polymer adsorbents were added to the solution medium and the solution was mixed at constant rpm in a rotary shaker for 24 hours. At the end of these processes, the suspension was filtered and the filtrate was analyzed using an ICP-MS device. Since there are no mercury, antimony, arsenic ions in the commercial mix-solution, the same procedures were repeated separately for the solution containing mercury ions. For the calibration graph, standards were prepared as 1;2,5;5;10;25;50, and 100 ppb from the standard solution and introduced to the device.

3. Results and Discussion

The structural characterization of the synthesized polymeric adsorbents in the study was carried out using FT-IR and ^{1}H-NMR spectroscopy. Surface appearances and elemental analyzes were made with SEM-EDX and XPS. Thermal stability and thermal behavior were investigated using DTA and TG. Adsorption studies were performed with ICP-MS. According to the results

obtained, the $PA_1M_1V_3$ derivative from the terpolymer selectively gave the best metal adsorption response and analyses were performed for this derivative.

3.1. FT-IR Analysis

Figure 2 shows the FT-IR spectra of the terpolymers. The most obvious difference between the polymer and monomer spectra is that the slightly low-intensity aliphatic pi bonds on the monomer units are broken and not seen in the polymer spectra. The carbonyl group that is absent in the VIm and Ap monomers is present in the MMA monomer, and therefore, seeing the carbonyl group at approximately 1740 cm^{-1} in the three different polymer derivatives supports the presence of MMA in the polymer mixture. C-N stretching peak of the VIm monomer was observed in all polymer derivatives at approximately 1450 cm^{-1}. Aromatic ring vibrations of the benzene ring in the Ap monomer can be seen in the range of about 1400-1500 cm^{-1} in PAMV polymers. In addition, the -C-H- stretching in the benzene ring is also seen in the terpolymer at 2900-3050 cm^{-1}. These results support that all monomer types are found in polymer derivatives [24, 25].
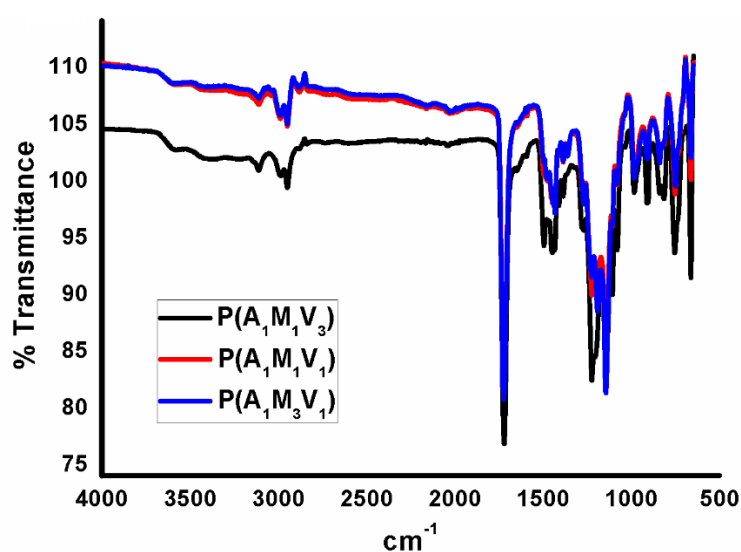
Figure 2. FTIR spectra of $PA_1M_1V_3$, $PA_1M_1V_1$, $PA_1M_3V_1$ polymers

3.2. ^{1}H-NMR Analysis

In Figure 3, the ^{1}H-NMR spectrum of $PA_1M_1V_3$, one of the synthesized polymers, is shown as an example. Other derivatives $PA_1M_1V_1$ and $PA_1M_3V_1$ have a similar appearance with varying peak intensities and ^{1}H-NMR spectra belong to these terpolymers are shown in Figure 4. According to Figure 3, the aromatic proton peaks on allyl phenol are between 6.5-7.2 ppm, and the peaks of the methoxy group (-OCH$_3$) on methyl methacrylate are between 3.1-3.5 ppm [26]. The proton peak attached to the phenolic hydroxyl group on the allyl phenol was ~9.2 ppm. Proton peaks on the imidazole ring are between 7-8 ppm, as expected. The aliphatic proton peak

attached to the ring of imidazole is around 3.8-4 ppm [27]. The aliphatic group protons (-CH_2, -CH_3) in the polymer chain are clear between 1-2 ppm.
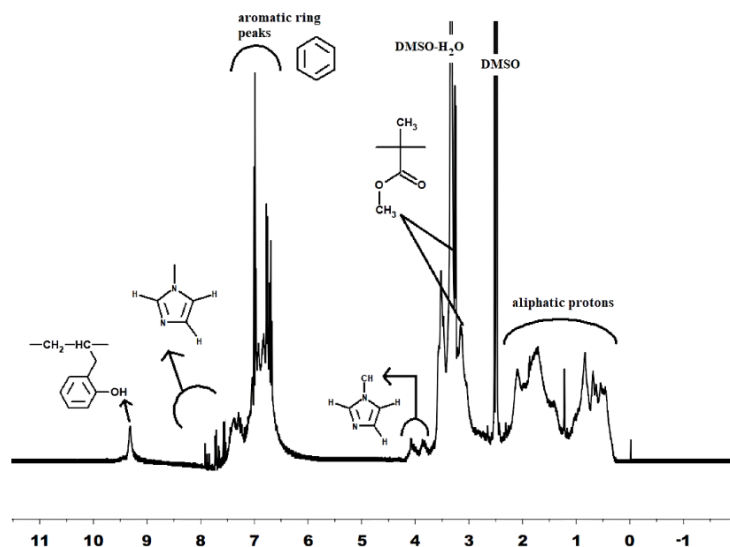
Figure 3. Annotated ^{1}H-NMR spectrum of $PA_1M_1V_3$ polymer
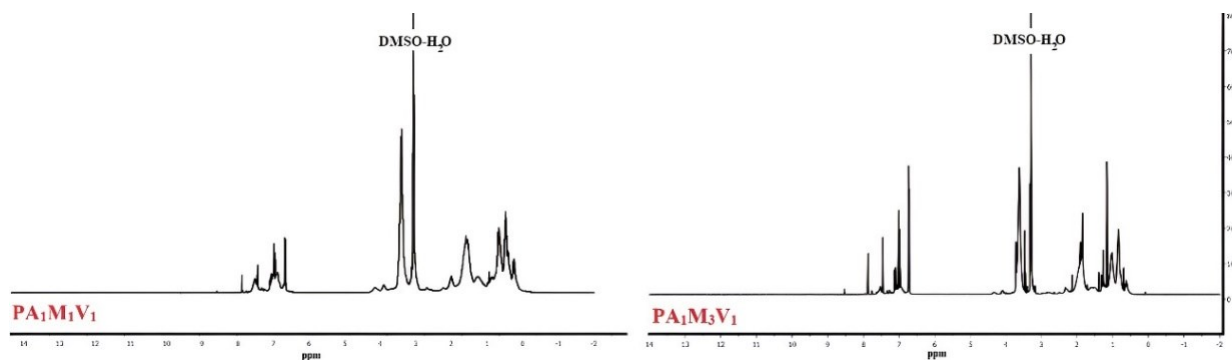
Figure 4. ^{1}H-NMR spectra of $PA_1M_1V_1$ and $PA_1M_3V_1$ polymer

3.3. SEM-EDX Analysis

Figure 5 shows the comparative SEM images of PAMV terpolymers. As is known, SEM images of MMA and VIm monomers are spherical [28 ,29]. Allylphenols are expected to have a more planar appearance. In Figure 5, $PA_1M_1V_3$ polymer has a spherical appearance due to the high percentage of VIm monomer. In $PA_1M_1V_1$ polymer, where all monomer components are reacted equally in moles, planar appearance and spherical appearance are seen together. In the $PA_1M_3V_1$ polymer, where the methyl methacrylate monomer is mole-dense, the large spherical appearance is more prominent. This image supports that MMA is found more frequently in polymer chains. In general, the SEM images were as expected in accordance with the literature.

EDX analysis was also performed with SEM. Figure 6 and Table 3 show EDX results and atomic percentages, respectively.

The experimental results obtained are in agreement with the theoretically calculated atomic percentages. As can be seen from the data in Table 3, the highest nitrogen atom percentage is in the $PA_1M_1V_3$ polymer as expected and is very close to the theoretical calculation. The derivative with the highest number of oxygen atoms is the $PA_1M_3V_1$ polymer where the MMA monomer is expected to be higher in moles. In general, when the theoretical and experimental results are followed, it can be said that the percentage of carbon atoms is lower than the theoretical calculation and the percentage of oxygen atoms is higher. This is because the polymerization kinetics of methyl methacrylate are higher than those of other VIm and Ap monomers. In this case, MMA was more incorporated into the polymer chains and the number of oxygen atoms was generally higher than expected. For the same reason, the nitrogen atom and the carbon atom have a lower percentage.
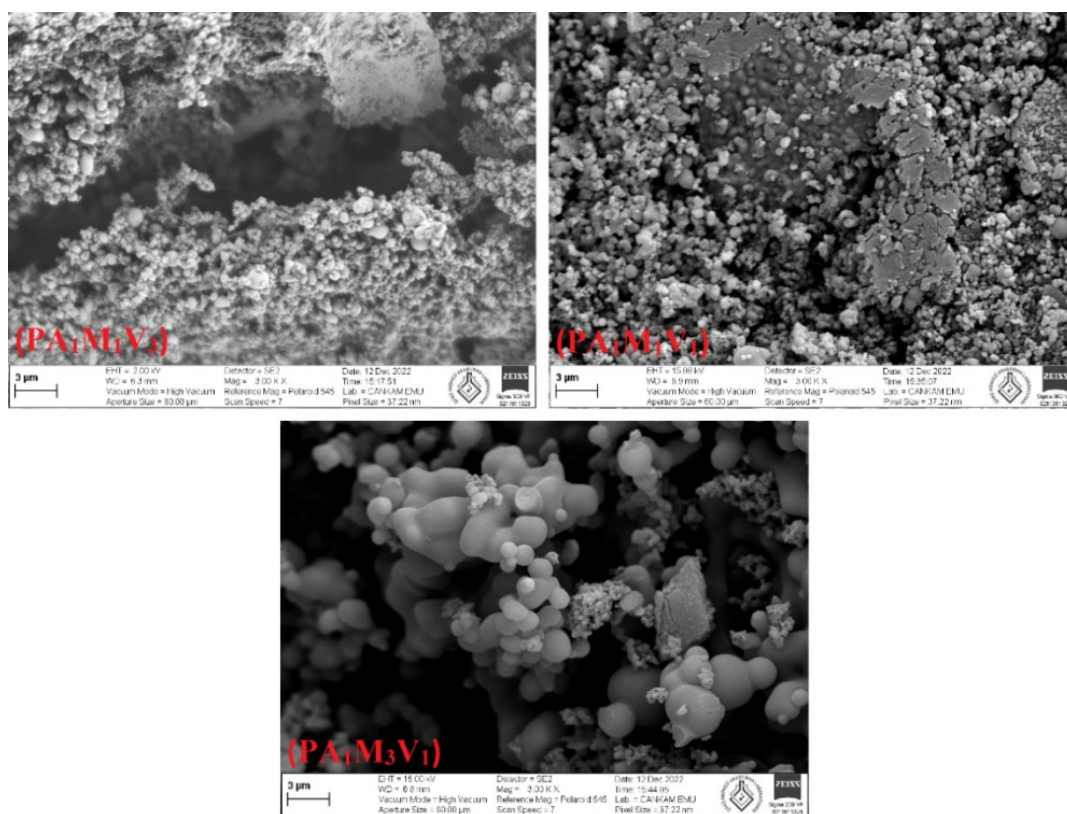
Figure 5. SEM images of $PA_1M_1V_3$, $PA_1M_1V_1$ and $PA_1M_3V_1$ polymers
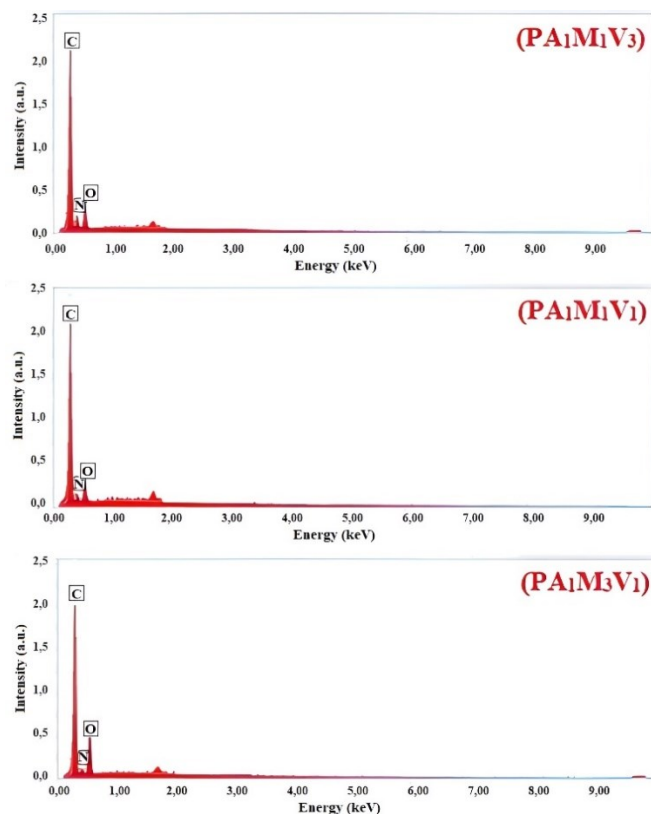
Figure 6. EDX analyses of $PA_1M_1V_3$, $PA_1M_1V_1$ and $PA_1M_3V_1$ polymers

Table 3. Elemental analysis results of PAMV adsorbents

Element	$(PA_1M_1V_3)$ Atomic %		$(PA_1M_1V_1)$ Atomic %		$(PA_1M_3V_1)$ Atomic %	
	Experimental	Theoric	Experimental	Theoric	Experimental	Theoric
C	69.01	76.3	74.81	79.2	69.44	76.3
N	16.30	15.8	10.98	8.3	6.65	5.2
O	14.69	7.9	14.21	12.5	23.91	18.5

3.4. Thermal Analysis

Thermal behavior of PAMV polymer derivatives was investigated by TG, DTG and DTA analyses. In Figure 7, TG and DTG curves of $PA_1M_1V_1$, $PA_1M_1V_3$ and $PA_1M_3V_1$ polymers are given comparatively, DTA analyses are given collectively in Figure 8. When we examine the TG and DTG curves in Figure 7, it can be seen that two main degradation steps occur in the $PA_1M_1V_3$ derivative, which is the derivative with high moles of vinyl imidazole. The maximum decomposition temperatures of these steps were approximately $Tmax_1$ 270 °C and $Tmax_2$ 425 °C, respectively. It is thought that the first break in the polymer chain is caused by the vinyl imidazole segment, and the break after the MMA segment. The most thermally stable derivative

is the $PA_1M_3V_1$ derivative. The reason for this is the high amount of methyl methacrylate monomer in the chain. It is known that PMMA gives a decomposition step around 400 ºC. The $PA_1M_3V_1$ polymer has one degradation step and has a Tmax of about 430 ºC. The thermal stability of the $PA_1M_1V_1$ polymer derivative was between those of the other two derivatives [30]. There were two decay steps. The maximum decomposition temperatures were approximately 350 ºC and 412 ºC, respectively. The decomposition step with a maximum temperature of 350 ºC may result from oxidative decomposition of the aromatic ring.

When the DTA diagrams in Figure 8 are examined, an endothermic peak is observed in the $PA_1M_1V_3$ derivative, depending on the glass transition temperature of the Polyvinyl imidazole chains between 60 ºC and 70 ºC [31]. In $PA_1M_1V_1$ and $PA_1M_3V_1$ derivatives, this transition occurs between 100-120 ºC and 130-160 ºC, respectively [32]. This change depended on the percentage of PMMA in the terpolymer chains. The endothermic peak observed at approximately 207-275 °C for all three derivatives was attributed to aromatic ring breakage [33].
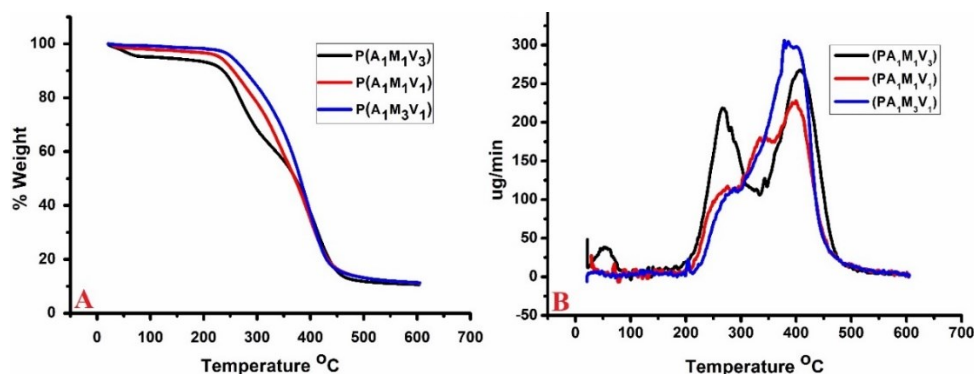
Figure 7. TG and DTG curves of $PA_1M_1V_3$, $PA_1M_1V_1$ and $PA_1M_3V_1$ polymers
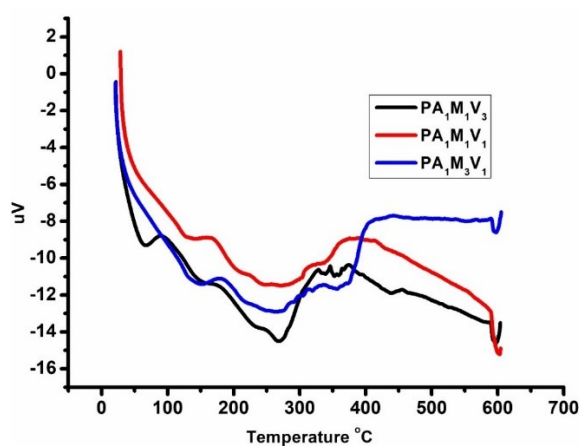
Figure 8. DTA curves $PA_1M_1V_3$, $PA_1M_1V_1$ and $PA_1M_3V_1$ polymers

3.5. XPS Analysis

Diagrams showing the bonding energies of carbon, nitrogen and oxygen atoms obtained from XPS analysis of PAMV polymer adsorbents are given in Figure 9. In Table 4, the binding energies of each derivative in eV and the atomic percentages of the elements are given in detail. According to the data from the XPS analysis, the N1s spectra in the imidazole ring are decomposed into two peaks of 398.6-398.9 and 400.53-400.78. These peaks are caused by the sp3 ($(CH)_3$-N) and sp^2 (C=N-) bonds of nitrogen, and the peak intensities are expected to be close to each other. The derivative with the highest percentage of nitrogen atoms in polymers is in the $PA_1M_1V_3$ derivative, as it should, because theoretically, this derivative has the highest moles of vinylimidazole. However, as in the EDX analysis, because of the polymerization kinetics of 1-vinylimidazole and allyl phenol are not as fast as methyl methacrylate, nitrogen the percentage is slightly lower than expected. Chemical shifts of C1s XPS spectra in all PAMV polymer adsorbents were observed in three different regions which are at about 285.2, 286.5, and 288. 9 eV. The C=O bond interaction in the carbonyl group is characteristically moderate at approximately 288.9 eV in all three polymer derivatives. The C-C binding energy was determined as a high-intensity peak at approximately 285 eV [34, 35]. C-N and C-O binding energies are seen in almost the same energy region at 286 eV in polymeric structures [36]. Consistent with this result, a moderate peak at 286.5 is clearly seen in all PAMV derivatives. These observed binding energies support the presence of MMA, VIm, and Ap monomers in the terpolymer. As expected, when looking at the atomic percentages, the derivative with the highest nitrogen content was $PA_1M_1V_3$ (9.18%). The percentages of $PA_1M_1V_1$ and $PA_1M_3V_1$ derivatives are 4.33 and 3.38, respectively. Although these rates are consistent within themselves, they are slightly lower than the theoretically calculated values. This may be due to point analysis of the samples and the random distribution of monomer units in the chains rather than sequentially.
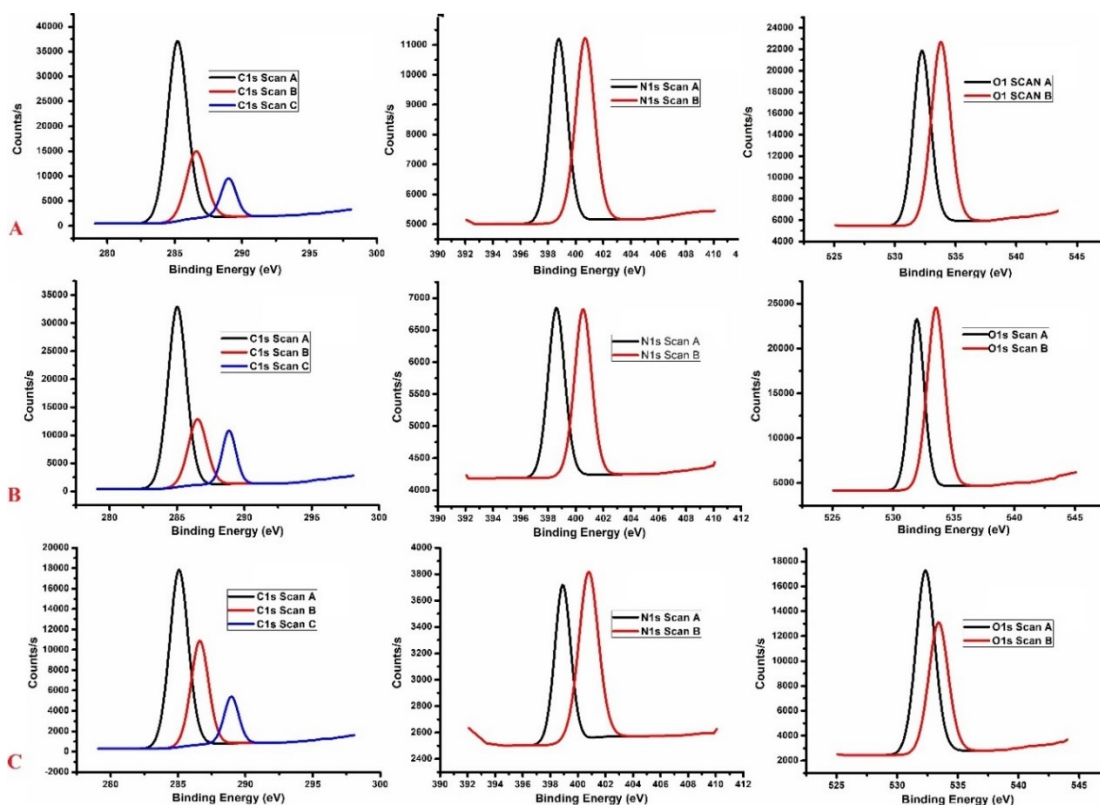
Figure 9. C1s, N1s and O1s XPS scan of $PA_1M_1V_3(A)$, $PA_1M_1V_1(B)$ and $PA_1M_3V_1(C)$ polymers

Table 4. XPS scanning of C1s, N1s, O1s atoms and atomic percentages

Element Scan Name	$PA_1M_1V_3$		$PA_1M_1V_1$		$PA_1M_3V_1$	
	Peak BE (eV)	Atomic %	Peak BE (eV)	Atomic %	Peak BE (eV)	Atomic %
C1s Scan A	285.21	47.48	285.02	46.24	285.07	39.64
C1s Scan B	286.59	17.31	286.52	16.74	286.61	21.78
C1s Scan C	288.99	7.82	288.86	10.27	288.95	8.23
N1s Scan A	398.77	4.42	398.6	2.16	398.9	1.47
N1s Scan B	400.69	4.76	400.53	2.17	400.78	1.91
O1s Scan A	532.22	8.52	531.96	10.04	532.32	15.56
O1s Scan B	533.78	9.68	533.53	12.38	533.4	11.4

3.6. ICP-MS Analyses

Because the metal adsorption results of $PA_1M_1V_3$ from PAMV derivatives gave the best results, the study of this derivative is presented. The adsorption percentages of terpolymers prepared

with similar monomers in the literature are close to this study. However, while this polymer was synthesized in multiple steps, at high temperatures and using excess reactant, the $PA_1M_1V_3$ derivative polymer was produced in a single step, at room temperature and in a solvent-free environment, by photopolymerization, an environmentally friendly method [37, 38].

Adsorption measurements were carried out for 19 different elements at five different pH values, pH=2, 4, 6, 8, and 10. The metals investigated were B, Mg, Al, Ca, Cr, Mn, Fe, Co, Ni, Cu, Zn, As, Sr, Cd, Sb, Ba, Hg, Tl and Pb. It was determined that polymeric adsorbent best responded to which heavy metals with high toxic effect. According to the results obtained, the toxic metals with selective and highest adsorption at different pH values are chromium (Cr), cadmium (Cd) and mercury (Hg). According to the ICP-MS results, the sorption of the synthesized terpolymer (PAMV) at different pH values, especially iron (Fe), copper (Cu) and lead (Pb), is quite remarkable. In Table 5, the sorption results of the studied metals are given and they show the amount of metal remaining in the solutions after adsorption in ppb. The results seen in table 5 show that the terpolymer can be used selectively in sensor studies. The sorption percentages for cadmium, chromium, mercury metals and the graphs of sorption percentages against pH are shown in Table 6 and Figure 10, respectively.

From the results obtained, the zeta potential of the PAMV terpolymer was calculated by the pH_i-pH_f method [39]. For this, the final pH_f values of the solutions were determined after filtration and the necessary data were plotted. Figure 11 and Table 7 show these data. According to the data obtained, the pH_{pzc} value of $PA_1M_1V_3$ adsorbent is ~6.
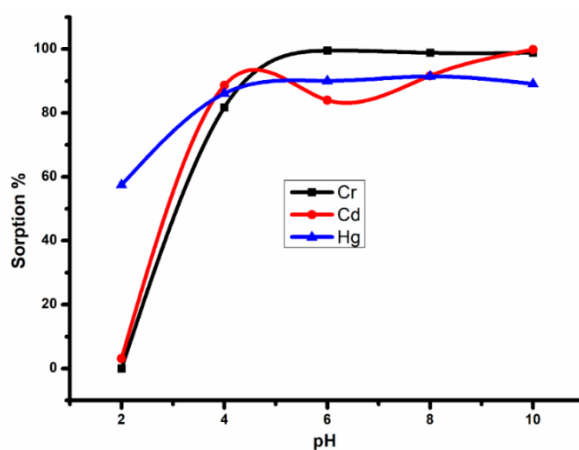
Figure 10. The sorption percentages of Cr, Hg and Cd ions of $PA_1M_1V_3$ polymeric adsorbent at pH=2, 4, 6, 8 and 10
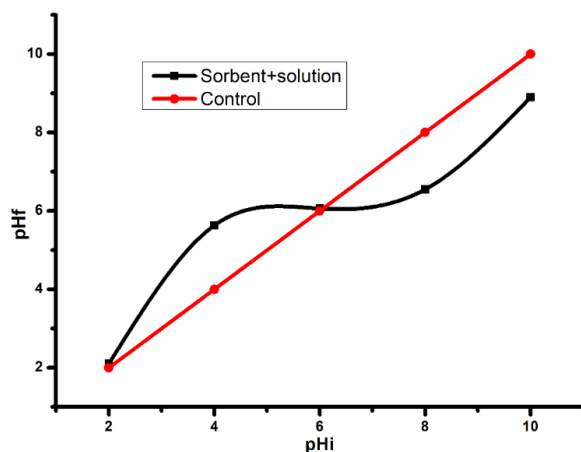
Figure 11. Determination of initial (pHi) and final (pHf) pH values and pHpzc value of PA$_1$M$_1$V$_3$ polymer adsorbent

Table 5. Metal amounts (ppb) read after adsorption of PA$_1$M$_1$V$_3$ adsorbent at different pH

	pH	43 Cr	55 Mn	56 Fe	59 Co	60 Ni	63 Cu	66 Zn	111 Cd	201 Hg	206 Pb	207 Pb	208 Pb
		Metal amounts remaining after adsorption (ppb)											
PA$_1$M$_1$V$_3$	2	100	100	100	100	100	100	100	96	42	90	90	90
	4	18	43	25	32	23	13	27	11	13	3	3	3
	6	0.4	45	7	33	23	0.5	24	15	9	5	5	5
	8	1.1	44	5	29	9	0.7	19	8	8	22	20	21
	10	1.1	1.8	4	3	3	1.1	0.7	0.1	10	2	2	2

Table 6. The sorption percentages of Cr, Cd, Hg metal ions at different pHs of the PA$_1$M$_1$V$_3$ adsorbent

pH	Cr		Cd		Hg	
	Cf	%S	Cf	%S	Cf	%S
2	100.000	0	96.908	3.092	42.529	57.471
4	18.249	81.751	11.318	88.682	13.902	86.098
6	0.498	99.502	15.975	84.025	9.952	90.048
8	1.188	98.812	8.380	91.620	8.584	91.416
10	1.193	98.807	0.180	99.820	10.907	89.093

Table 7. PH_f value and pH_{pzc} value of $PA_1M_1V_3$ adsorbent

	pHi	pHf	pHpzc
	2	2.1	
	4	5.63	
PA₁M₁V₃	6	6.06	~6
	8	6.55	
	10	8.9	

4.   Conclusion

In this study, poly(allylphenol-co-methylmethacrylate-co-vinyl imidazole) (PAMV) polymeric adsorbents were successfully synthesized by photopolymerization, which is a solvent-free and temperature-free green method that uses VIm, Ap and MMA monomers. A low-cost, short and easily produced adsorbent with selective adsorption capacity, primarily mercury (II), chromium (III) and cadmium (II) ions in wastewater or aqueous solutions has been synthesized. The results showed, that the polymeric adsorbent reached a higher metal holding capacity in the basic region. The zeta potential was determined to be 6 in the pH_{pzc} measurement based on the first and last pH measurements. The presence of monomers in the structure was determined using XPS and EDX analyses and their percentages in the chain were compared theoretically and experimentally. The obtained results show that there is high potential for obtaining a useful adsorbent with advanced analytical techniques and applications.

Ethics in Publishing

There are no ethical issues regarding the publication of this study.

References

[1] Ahmed, S., Akhtar, N., Rahman, A., Mondal, N.C., Khurshid, S., Sarah, S., Khan, M.A.K., Kamboj, V. (2022) Evaluating groundwater pollution with emphasizing heavy metal hotspots in an urbanized alluvium watershed of Yamuna River, northern India. Environmental Nanotechnology, Monitoring and Management, 18, 100744.

[2] Kumar, S., Prasad, S., Yadav, K.K., Shrivastava, M., Gupta, N., Nagar, S., Bach, Q., Kamyab, H., Khan, S., Yadav, S., Malav, L. (2019) Hazardous heavy metals contamination of

vegetables and food chain: Role of sustainable remediation approaches-A review. Environmental Research, 179, 108792.

[3] Islam, M.S., Ismail, Z., Jamal, M.H., Ibrahim, Z., Jumain, M., Islam, T. (2022) Heavy metals from different land use soil in the capital of ancient Pundranagar, Bangladesh: a preliminary study for ecological risk assessment. Chemistry and Ecology, 38 (8), 720-743.

[4] Du, J., Zhang, B., Li, J., Lai, B. (2020) Decontamination of heavy metal complexes by advanced oxidation processes: A review. Chinese Chemical Letters, 31, 2575–2582.

[5] Zheng, M., Sun, Z., Han, H., Zhang, Z., Ma, W. Xu, C. (2021) Enhanced coagulation coupled with heavy metal capturing for heavy metals removal from coal gasification brine and a novel mathematical model. Journal of Water Process Engineering, 40, 101954.

[6] Gunarathne, V., Rajapaksha, A.U., Vithanage, M., Alessi, D.S., Selvasembian, R. Naushad, M., You, S., Oleszczuk, P., Ok, Y.S. (2022) Hydrometallurgical processes for heavy metals recovery from industrial sludges. Critical Reviews in Environmental Science and Technology, 52 (6), 1022-1062.

[7] Zhang, Y., Duan, X. (2020) Chemical precipitation of heavy metals from wastewater by using the synthetical magnesium hydroxy carbonate. Water Science and Technology, 81 (6), 1130-1136.

[8] Jia, L., Liu, H., Kong, Q., Li, M., Wu, S., Wu, H. (2020) Interactions of high-rate nitrate reduction and heavy metal mitigation in iron-carbon-based constructed wetlands for purifying contaminated groundwater. Water Research, 169, 115285.

[9] Bashir, A., Malik, L.A., Ahad, S., Manzoor, T., Bhat, M.A., Dar, G.N., Pandith, A.N. (2019) Removal of heavy metal ions from aqueous system by ion exchange and biosorption methods. Environmental Chemistry Letters, 17, 729–754.

[10] Saltan, F., Murat Saltan, G. (2022) Synthesis of a new adsorbent poly(allylisothiocyanate-co-hydroxyethylmethacrylate-co-vinylimidazole) via photopolymerization: Characterization and investigation of heavy metal adsorption capacity. Journal of Applied Polymer Science, 139, e52639.

[11] Qiu, B., Tao, X., Wang, H., Li, W., Ding, X. Chu, H. (2021) Biochar as a low-cost adsorbent for aqueous heavy metal removal: A review. Journal of Analytical and Applied Pyrolysis, 155, 105081.

[12] Sheth, Y., Dharaskar, S., Khalid, M., Sonawane, S. (2021) An environment friendly approach for heavy metal removal from industrial wastewater using chitosan based biosorbent: A review. Sustainable Energy Technologies and Assessments, 43, 100951.

[13] Bhatt, R.R., Shah, B.A. (2015) Sorption studies of heavy metal ions by salicylic acid–formaldehyde–catechol terpolymeric resin: Isotherm, kinetic and thermodynamics. Arabian Journal of Chemistry, 8, 414–426.

[14] Sidharaj, N., Rajarajan, G., Senthil, M., Velmurugan, G. (2022) Synthesis, characterization and applications: Novel terpolymer and its composite. Materials Today: Proceedings, 59, 309–315.

[15] Velmurugan, G., Ahamed, K.R., Azarudeen, R.S. (2015) A novel comparative study: synthesis, characterization and thermal degradation kinetics of a terpolymer and its composite for the removal of heavy metals. Iranian Polymer Journal, 24, 229–242.

[16] Azarudeen, R.S., Subha, R., Jeyakumar, D., Burkanudeen, A.R. (2013) Batch separation studies for the removal of heavy metal ions using a chelating terpolymer: Synthesis, characterization and isotherm models. Separation and Purification Technology, 116, 366–377.

[17] Saltan, F. (2021) Preparation of poly(eugenol co methyl methacrylate)/polypropylene blend by creative route approach: structural and thermal characterization. Iranian Polymer Journal, 30, 1227–1236.

[18] Soykan, U., Öztoprak, B. (2020) A Yield Study on Self-Initiated Photopolymerization of Acrylate Monomers Bearing Benzophenone Pendant Unit. Journal of New Results in Science, 9, 1-8.

[19] Temel, G., Karaca, N., Arsu, N. (2010) Synthesis of Main Chain Polymeric Benzophenone Photoinitiator via Thiol-ene Click Chemistry and Its Use in Free Radical Polymerization. Journal of Polymer Science Part A-Polymer Chemistry, 48, 5306-5312.

[20] Arasaretnam, S., Dilshani Jayarathna, U.P. (2020) Synthesis, Characterization, and Metal Adsorption Properties of Formaldehyde-Based Terpolymeric Resins Derived from Anthranilic Acid, Salicylic Acid, and Catechol. Journal of Chemistry, 2020, 8843162.

[21] Pekel, N., Güven, O. (1999) Investigation of complex formation between poly(N-vinyl imidazole) and various metal ions using the molar ratio method. Colloid and Polymer Science, 277, 570-573.

[22] Fujisawa, S., Atsumi, T., Kadoma, Y., Sakagami, H. (2002) Antioxidant and prooxidant action of eugenol-related compounds and their cytotoxicity. Toxicology, 177 (1), 39-54.

[23] Nenadis, N., Papapostolou, M., Tsimidou, M.Z. (2021) Suggestions on the Contribution of Methyl Eugenol and Eugenol to Bay Laurel (Laurus nobilis L.) Essential Oil Preservative Activity through Radical Scavenging. Molecules, 26, 2342.

[24] Poljanšek, I., Krajnc, M. (2005) Characterization of Phenol-Formaldehyde Prepolymer Resins by In Line FT-IR Spectroscopy. Acta Chimica Slovenica, 52 (3), 238–244

[25] Murugan, E., Jebaranjitham, J.N. (2012) Synthesis and characterization of silver nanoparticles supported on surface-modified poly(N-vinylimidazale) as catalysts for the reduction of 4-nitrophenol. Journal of Molecular Catalysis A: Chemical, 365, 128–135.

[26] Wu, K.H., Tsai, C.W., Huang, W.C., Hung, W.C. (2021) Structural design and characterization of tricycloalkyl-containing methacrylate with methyl methacrylate copolymers. Materials Science and Engineering B, 267, 115088.

[27] Farrokhi, M., Abdollahi, M. (2020) Enhancing medium/high temperature proton conductivity of poly (benzimidazole)-based proton exchange membrane via blending with poly (vinyl imidazole-co-vinyl phosphonic acid) copolymer: Proton conductivitycopolymer microstructure relationship. European Polymer Journal, 131, 109691.

[28] Navarchian, A.H., Najafipoor, N., Ahangaran, F. (2019) Surface-modified poly(methyl methacrylate) microcapsules containing linseed oil for application in self-healing epoxy-based coatings. Progress in Organic Coatings, 132, 288-297.

[29] Sanchez-Paniagua Lo´pez, M., Lo´pez-Cabarcos, E., Lo´pez Ruiz, B. (2009) Biosensors Based on Poly(vinylimidazole) Microparticles. Electroanalysis, 21 (3-5), 512–520.

[30] Gonçalves, G., Paula Marques, A.A.P., Barros-Timmons, A., Bdkin, I., Singh, M.K., Emami, N., Gracio, J. (2010) Graphene oxide modified with PMMA via ATRP as a reinforcement filler. Journal of Materials Chemistry, 20, 9927-9934.

[31] Camacho-Cruz, L.A., Velazco-Medel, M.A., Parra-Delgado, H., Bucio, E. (2021) Functionalization of cotton gauzes with poly(N-vinylimidazole) and quaternized poly(N-vinylimidazole) with gamma radiation to produce medical devices with pH-buffering and antimicrobial properties. Cellulose, 28, 3279–3294.

[32] Acevedo, B., Martınez, F., Olea, F. (2013) Synthesıs, Thermal Behavıor, and Aggregatıon in Aqueous Solutıon of Poly(Methyl Methacrylate)-b-Poly(2-Hydroxyethyl Methacrylate). Journal of the Chilean Chemical Society, 58 (4), 2038-2042.

[33] Liu, J., Li, R., Guo, M., Tao, H., Sun, D. Zong, C., Liu, C., Fu, F. (2017) Study of the thermal degradation of benzene-containing glycerol carbonate derivatives by a combined TG–FTIR and theoretical calculation. Thermochimica Acta, 654, 179-185.

[34] Zhao, M., Cao, Y., Liu, X., Deng, J., Li, D. Gu, H. (2014) Effect of nitrogen atomic percentage on N+-bombarded MWCNTs in cytocompatibility and hemocompatibility. Nanoscale Research Letters, 9, 142.

[35] Ranganathan, K., Morais, A., Nongwe, I., Longo, C., Nogueira, A.F. Coville, N.J. (2016) Study of photoelectrochemical water splitting using composite films based on TiO2 nanoparticles and nitrogen or boron doped hollow carbon spheres as photoanodes. Journal of Molecular Catalysis A: Chemical, 422, 165-174.

[36] Gavrielides, A., Duguet, T., Esvan, J., Lacaze-Dufaure, C., Bagus, P.S. (2016) A poly-epoxy surface explored by Hartree-Fock #SCF simulations of C1s XPS spectra. The Journal of Chemical Physics, 145, 074703.

[37] Culbertson, B.M., Post, L.K., Aulabaugh, A.E. (1983) Polymers derved from ally lephenol or substıtuted allylphenol and malec anhydrıde. United States Patent, 4, 388-451.

[38] Mu, S., Liu, W., Zhao, L., Long, Y., Gu, H. (2019) Antimicrobial AgNPs composites of gelatin hydrogels crosslinked by ferrocene-containing tetrablock terpolymer. Polymer, 169, 80-94.

[39] Cardenas-Peña, A.M., Ibanez, J.G., Vasquez-Medrano, R. (2012) Determination of the Point of Zero Charge for Electrocoagulation Precipitates from an Iron Anode. International Journal of Electrochemical Science, 7, 6142-6153.